International Journal of Microwave and Wireless Technologies

cambridge.org/mrf

Inferring the atmospheric duct from radar sea clutter using the improved artificial bee colony algorithm

Chao Yang[1] and Lixin Guo[2]

[1]School of Science, Xi'an University of Posts and Telecommunications, Xi'an, Shaanxi, China and [2]School of Physics and Optoelectronic Engineering, Xidian University, Xi'an, Shaanxi, China

Research Paper

Cite this article: Yang C, Guo L (2018). Inferring the atmospheric duct from radar sea clutter using the improved artificial bee colony algorithm. *International Journal of Microwave and Wireless Technologies* **10**, 437–445. https://doi.org/10.1017/S1759078718000247

Received: 10 September 2017
Revised: 23 January 2018
Accepted: 23 January 2018
First published online: 21 February 2018

Key words:
Artificial bee colony; atmospheric duct estimation; orthogonal crossover; orthogonal experimental design; radar sea clutter

Author for correspondence:
Chao Yang, E-mail: yang_chaomail@163.com

Abstract

In this paper, an orthogonal crossover artificial bee colony (OCABC) algorithm based on orthogonal experimental design is presented and applied to infer the marine atmospheric duct using the refractivity from clutter technique, and the radar sea clutter power is simulated by the commonly used parabolic equation method. In order to test the accuracy of the OCABC algorithm, the measured data and the simulated clutter power with different noise levels are, respectively, utilized to estimate the evaporation duct and surface duct. The estimation results obtained by the proposed algorithm are also compared with those of the comprehensive learning particle swarm optimizer and the artificial bee colony algorithm combined with opposition-based learning and global best search equation. The comparison results demonstrate that the performance of proposed algorithm is better than those of the compared algorithms for the marine atmospheric duct estimation.

Introduction

The lower atmospheric duct commonly encountered in marine boundary layer is an anomalous electromagnetic environment, which is caused by small changes of the index of refraction due to the sharp variation in the vertical atmospheric temperature and humidity above the sea surface. Hence, the performance of the radar system and the communication system that are designed to operate under standard atmospheric conditions with a typical slope of 0.118 M-units/s work in the non-standard environment may be greatly changed, such as the maximum operation range, creation of radar holes where the radar is practically blind, and strengthened sea surface clutter, etc [1, 2]. Clearly, accurate prediction of atmospheric environment is crucial for evaluating the performance of both the radar and communication systems in the marine environment.

Since the radar sea clutter is significantly changed by the atmospheric duct, in turn, radar sea clutter contains useful information on atmospheric environment, which makes it possible to determine refractivity from clutter (RFC) [3–5]. The RFC technique is widely used in the field of atmospheric duct estimation, which has the advantages of simple devices and low cost. Obviously, atmosphere duct estimation using RFC technique is an inverse problem, and the optimization algorithm can exactly find the best refractivity profile among the candidate profiles according to the objective function defined by the observed and simulated clutter power. The smaller the objective function value, the better match gets. The best refractivity profile corresponds to the minimum objective function value, and *vice versa*.

Gerstoft *et al.* estimated the atmospheric refractivity from radar sea clutter observations and provide the specific steps involved in RFC [4]. Karimian *et al.* provided the latest developments in RFC and the area that needs further investigation [5]. Yardim *et al.* applied a Markov chain Monte Carlo samplers to the estimation of the refractivity profile using radar clutter [6]. Vasudevan *et al.* utilized the recursive Bayesian estimation framework in the RFC [7]. Douvenot *et al.* adopted the least square support vector machine method to estimate the refractivity profile of the surface duct based on a pregenerated database [8]. Yardim *et al.* tracked the lower atmospheric refractivity with RFC [1]. Wang *et al.* employed the particle swarm optimization algorithm to retrieve the evaporation duct height [9]. Zhao *et al.* introduced the simulated annealing algorithm to study the atmospheric duct estimation problem [10]. Zhang *et al.* introduced a four-parameter modified refractivity profile model for the evaporation duct estimation with RFC [11]. The artificial bee colony (ABC) algorithm [12, 13] inspired by the intelligent foraging behavior of honey bee swarm is one of the most recently proposed bio-inspired swarm intelligence algorithm, and it is applied to the electromagnetic optimization problem [13] and atmospheric duct estimation [14, 15]. Yang employed the ABC to the atmospheric duct estimation, and the results showed that the performance of ABC is better than particle swarm optimizer according to the comparative analysis results

CAMBRIDGE UNIVERSITY PRESS

[14]. Yang *et al.* proposed the ABC algorithm combined with opposition-based learning and global best search equation (OGABC) to improve the problems of the slow convergence speed and sinking into local optima appear in the duct estimation problem, and investigation results indicate that the OGABC achieves good performance compared with the ABC and the modified invasive weed optimization [15].

Although there are certain improvements on the ABC, there is still room for seeking a balance between the exploration and exploitation. This is because that both exploration and exploitation are necessary for evolutionary algorithms, but the two aspects contradict to each other [16]. Owing to the search equation in ABC is good at exploration but poor at exploitation, an orthogonal crossover artificial bee colony (OCABC) algorithm based on orthogonal experimental design (OED) is proposed by incorporating the orthogonal crossover (OC) into ABC, which makes use of the OC to improve the search ability. In addition, a novel transmission vector, which will take part in the OCABC, is given to take the advantage of the information of global best solution to generate new candidate solutions with the purpose of enhancing the poor exploitation in ABC.

The forward problem and inverse problem model

The parameterized environmental model

In this paper, we focus on the inversion of the evaporation duct and surface duct estimation problem, and their refractivity profiles are shown in Fig. 1. Owing to the potential drawback of one parameter log-linear profile in describing the evaporation duct, the following four-parameter model is adopted [11]

$$M(z) = M_0 + kz \quad z \le z_{joint}, \tag{1}$$

$$M(z) = M_0 + (k - 0.125\rho_1)z_{joint} + 0.125\rho_1 z + 0.125\rho_1 d \ln\left(\frac{z_{joint} + z_0}{z + z_0}\right) z_{joint} < z < d, \tag{2}$$

$$M(z) = M_0 + (k - 0.125\rho_1)z_{joint} + 0.125(\rho_1 - \rho_2)d + 0.125\rho_2 z + 0.125d \ln\left[\frac{(z_{joint} + z_0)^{\rho_1}}{(d + z_0)^{\rho_1 - \rho_2} \cdot (z + z_0)^{\rho_2}}\right] \quad z \ge d, \tag{3}$$

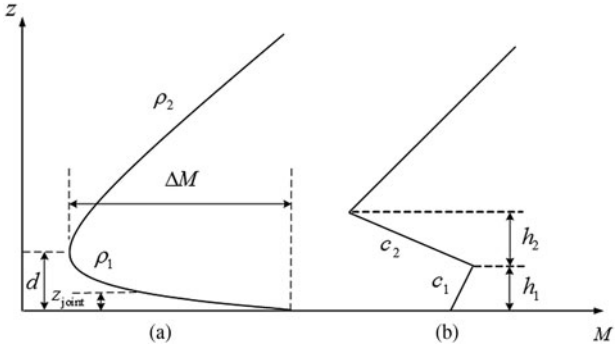

Fig. 1. The model of refractivity profile. (a) Four-parameter evaporation duct; (b) surface duct.

where M_0 is the base refractivity, k is the slope of the line, z is the height above the sea surface, d is the evaporation duct height, z_0 is the roughness factor usually taken as 0.00015, z_{joint} represents the specific height, ρ_1 and ρ_2 are the adjustment factors for the profile less and greater than d, respectively. It is noted that ΔM represents the evaporation duct strength, which is related to k by implicit equation (4)

$$\Delta M = (0.125\rho_1 - k)\left(\frac{d}{1 - 8k/\rho_1} - z_0\right) + 0.125\rho_1 d \ln[(d + z_0)(1 - 8k/\rho_1)/e/d]. \tag{4}$$

Once equation (4) is solved for k, the z_{joint} can be easily obtained by equation (5)

$$z_{joint} = \frac{d}{1 - 8k/\rho_1} - z_0, \; k \le 0. \tag{5}$$

Obviously, the four-parameter evaporation duct profile can be obtained by equations (1)–(5) and determined by the parameter vector $\boldsymbol{m} = (d, \Delta M, \rho_1, \rho_2)$.

The surface duct can be represented by the four-parameter trilinear refractivity profile [1]

$$M(z) = M_0 + \begin{cases} c_1 z & z < h_1 \\ c_1 h_1 + c_2(z - h_1) & h_1 \le z \le h_2 \\ c_1 h_1 + c_2 h_2 + 0.118(z - h_1 - h_2) & z > h_2 \end{cases}, \tag{6}$$

where c_1 and h_1 are the slope and thickness of the base layer, whereas c_2 and h_2 are the slope and thickness of the inversion layer. The slope of the top layer is treated as a constant at 0.118 M-units/m. Similarly, the surface duct refractivity profile can be described by the parameter vector $\boldsymbol{m} = (c_1, c_2, h_1, h_2)$.

The propagation model

The most commonly adopted method to calculate the over-the-horizon propagation of electromagnetic wave in the atmospheric duct is the split-step Fourier solution of parabolic equation due to its stability and accuracy. If the initial field $u(x_0, z)$ is given, the split-step Fourier solution is obtained by [17, 18]

$$u(x_0 + \Delta x, z) = e^{ik_0 \Delta x M(\boldsymbol{m}, z)10^{-6}} F^{-1}\left\{e^{(i\Delta x/2k_0)p^2} F[u(x_0, z)]\right\}, \tag{7}$$

where k_0 is the free-space wavenumber, M is the modified refractivity, $\boldsymbol{m}$ is the refractivity parameter vector used to describe the refractivity profile of the atmospheric duct, p is the transform variable, Δx is the distance interval, and F and F^{-1} are the Fourier transform and inverse Fourier transform, respectively.

Correspondingly, the propagation loss $L(x, \boldsymbol{m})$ and the radar sea clutter power $P_c^r(x, \boldsymbol{m})$ can be easily obtained by the following equations [4, 8]

$$L(x, \boldsymbol{m}) = 32.45 + 20\lg f + 20\lg x - 20\lg(\sqrt{x}|u(x, z)|), \tag{8}$$

https://doi.org/10.1017/S1759078718000247 Published online by Cambridge University Press

$$P_c^r(x, \boldsymbol{m}) = -2L(x, \boldsymbol{m}) + \sigma^\circ + 10\lg(x) + C, \tag{9}$$

where f denotes the frequency in MHz, x is the propagation distance, $u(x, z)$ represents the field distribution, σ° is the radar cross-section, C is a constant.

The objective function

To estimate the parameter vector $\boldsymbol{m}$, the following least squares objective function is used [4]

$$f_{obj}(\boldsymbol{m}) = \boldsymbol{e}^{\mathrm{T}}\boldsymbol{e}, \tag{10}$$

$$\boldsymbol{e} = \boldsymbol{P}_c^{obs} - \boldsymbol{P}_c^r(\boldsymbol{m}) - \hat{T}, \tag{11}$$

$$\hat{T} = \bar{\boldsymbol{P}}_c^{obs} - \bar{\boldsymbol{P}}_c^r(\boldsymbol{m}), \tag{12}$$

where $\boldsymbol{P}_c^{obs}$ and $\boldsymbol{P}_c^r(\boldsymbol{m})$ stand for the observed and received clutter power at different ranges, and the bar stands for the mean across the elements.

Basic ABC algorithm

The ABC algorithm proposed by Karaboga and Basturk [12] is a relatively new swarm optimization algorithm, which simulates the foraging behavior of honey bee swarm. In ABC, a colony contains three types of bees: employed bees, onlooker bees, and scouts. The employed bees find the food sources and share the valuable information with onlooker bees. The onlooker bees in the hive need to choose the excellent food sources according to the information gathered by the employed bees. A food source is abandoned by the employed bee when its quality cannot be improved through a predetermined condition, and the employed bee becomes a scout. Then, the corresponding food source is randomly replaced by a new food source in the vicinity of the hive.

In ABC, a food source position stands for a possible solution of the optimization problem and the nectar amount of each food source represents the corresponding fitness. In ABC, first half of the colony is treated as the employed bees and the second half is called the onlookers, and the number of the employed bees or the onlookers is equal to the number of food source in the colony.

In the initialization phase, ABC generates a randomly distributed initial population. Each initial solution $X_i = [x_{i,1}, x_{i,2}, \ldots, x_{i,D}]$ is given by

$$x_{i,j} = x_{min,j} + rand(0, 1)(x_{max,j} - x_{min,j}), \tag{13}$$

where $i = 1, 2, \ldots, SN, j = 1, 2, \ldots, D$, SN is the number of the solutions and D is the dimension of the optimization problem; $rand(0, 1)$ represents a uniformly distributed random number in the range $(0, 1)$, $x_{min,j}$ and $x_{max,j}$ are the lower and upper bounds of the jth dimension, respectively.

In the employed bee phase, a new candidate solution V_i is generated by the old one X_i according to the following equation

$$v_{i,j} = x_{i,j} + \phi_{i,j}(x_{i,j} - x_{k,j}), \tag{14}$$

where $j \in \{1, 2, \ldots, SN\}$ and $k \in \{1, 2, \ldots, SN\}$ are randomly chosen indices and satisfy $i \neq k$, $\phi_{i,j}$ is a uniform random number in the range $(-1, 1)$.

In the onlooker phase, the food source is selected according to the probability value p_i related to the employed bees

$$p_i = \frac{fit_i}{\sum_{j=1}^{SN} fit_j}, \tag{15}$$

where fit_i is the fitness value of the solution i. In addition, the chosen food source position is updated by equation (14) to produce a new candidate food source. A greedy selection method is utilized to choose the better food source between the old and the new one in the employed bee phase and the onlooker bee phase.

In the scout phase, if a food source cannot be improved further through a predetermined parameter, called *limit*, it is abandoned and should be replaced by a new food source using equation (13). Then, the corresponding employed bee becomes a scout.

THE OCABC algorithm

The performance of evolutionary algorithms can be greatly improved by the OC since OED may be a powerful tool to discover the useful information from each food source's previous search experiences and utilize the valuable information to find an excellent candidate solution [19–23]. In the following, an improved ABC named OCABC is proposed based on OED.

Orthogonal experimental design

The orthogonal array (OA) is the core in the OED. With the help of an OA, the best combination may be obtained by testing a small number of well-representative experimental cases. Let $L_M(Q^N)$ stands for an OA with N factors and Q levels per factor, and L represents the OA and M is the number of combinations of levels. The estimation problem in this paper is a four-parameter inverse problem, so the $L_9(3^4)$ OA [19–23] is suitable

$$L_9(3^4) = \begin{bmatrix} 1 & 1 & 1 & 1 \\ 1 & 2 & 2 & 2 \\ 1 & 3 & 3 & 3 \\ 2 & 1 & 2 & 3 \\ 2 & 2 & 3 & 1 \\ 2 & 3 & 1 & 2 \\ 3 & 1 & 3 & 2 \\ 3 & 2 & 1 & 3 \\ 3 & 3 & 2 & 1 \end{bmatrix}. \tag{16}$$

In $L_9(3^4)$, there are four factors, three levels per factor and nine combinations of levels. Each row in $L_9(3^4)$ denotes a combination of levels, namely, a test. The OA in equation (16) has four columns, meaning that it is suitable for the estimation problem with at most four-parameter.

Orthogonal crossover

The OC is first introduced by Leung and Wang, and it works on two parent solutions $\boldsymbol{r} = (r_1, \ldots, r_D)$ and $\boldsymbol{t} = (t_1, \ldots, t_D)$. Thus, the corresponding solution range is defined by [20]

$$\boldsymbol{l} = [\min(r_1, t_1), \min(r_2, t_2), \ldots, \min(r_D, t_D)], \tag{17}$$

https://doi.org/10.1017/S1759078718000247 Published online by Cambridge University Press

$$\boldsymbol{u} = [\max(r_1, t_1), \max(r_2, t_2), \ldots, \max(r_D, t_D)]. \quad (18)$$

Evidently, the solution range for x_i is $[l_i, u_i] = [\min(r_i, t_i), \max(r_i, t_i)]$. Now, we quantize the i^{th} dimension of $(\boldsymbol{l}, \boldsymbol{u})$ into Q levels

$$l_{i,j} = l_i + \frac{j-1}{Q-1}(u_i - l_i) \quad j = 1, \ldots, Q. \quad (19)$$

The solution range defined by $\boldsymbol{r}$ and $\boldsymbol{t}$ will have Q^D points after quantization since each factor has Q possible values. Here, we take the $L_9(3^4)$ OA mentioned above as an example to explain the advantages of OED. Although it has 3^4 feasible solutions after quantization, only nine high-quality representative points that scattered uniformly over the solution range are tested to reduce the amount of computation and choose the best individual.

The OC operator based on OED is a powerful search tool, which is employed to find a promising candidate solution by combining the information of X_i and T_i. In this paper, the vector X_i is randomly selected from the current population and T_i is a transmission vector.

In order to enhance the poor exploitation ability of ABC and make a balance between the exploration and exploitation ability, a novel transmission vector T_i is constructed via the following equation

$$T_i = X_{best} + rand(0, 1) \cdot (X_{r1} - X_{r2}), \quad (20)$$

where X_{best} is the global best solution, the subscripts r_1 and r_2 are different indices uniformly randomly selected from (1, SN) and satisfy $r_1 \neq r_2 \neq i$. In equation (20), $rand(0, 1)$ is used to add more variation to the optimization process, and X_{best} is employed to improve the poor exploitation ability in ABC.

It should be noted that the computation cost will rapidly increase from SN to $SN \times (M + 1)$ at the employed bee stage if the OC operator is applied to each food source X_i. Hence, it is unwise to perform the OC operator on each pair of X_i and T_i at each generation. In this paper, the OC is executed five times at each generation to reduce the computation cost and improve the performance of the algorithm.

The procedures of OCABC

Since the search equation of ABC is good at exploration but poor at exploitation, the improved ABC named OCABC algorithm based on OC is proposed. The OC is used to discover the good information from X_i and T_i to produce an excellent candidate solution V_i, and the information of global best solution in the transmission vector can strengthen the exploitation ability and accelerate convergence. The main steps of OCABC are summarized below:

Step 1 Set the parameters and initialize the population;

Step 2 Randomly choose a small number of indices from (1, SN) to form a index vector o, where SN is the number of food sources;

Step 3 At the employed bee stage

Step 3.1

If i is not equal to one of the elements in the index vector o

Step 3.1.1 Generate a candidate food source V_i by the search equation (14) in ABC;

Else

Step 3.1.2 Generate a vector $T_{o(k)}$ by equation (20) and a suitable $L_M(Q^N)$ OA;

Step 3.1.3 Perform the OC operator on $T_{o(k)}$ and $X_{o(k)}$ to produce M tested candidate food sources $Z_j(1 \leq j \leq M)$ according to the OA generated in **Step 3.1.2**;

Step 3.1.4 Evaluate each of the tested candidate food source $Z_j(1 \leq j \leq M)$ and find the best candidate food source Z_b, namely, the $V_{o(k)}$;

Step 3.2 Select the better food source between X_i and $V_{o(k)}$;

End

Step 4 At the onlooker bee stage

Step 4.1 Update the position of food sources;

Step 4.2 Select the better food source again.

Step 5 Memorize the best solution so far.

Step 6 At the scout stage

The food source is replaced by a new random solution when the trial counter exceeds the *limit*.

Step 7 Repeat **Step 2** to **Step 6** until a terminating condition is reached.

Results and discussion

In the following, the OCABC is applied to the atmospheric duct estimation problem with the RFC technique, and the results of OCABC are compared with those of the comprehensive learning particle swarm optimizer (CLPSO) [24] and the OGABC [15]. Firstly, the measured data collected in East China Sea [9] are utilized to test the accuracy of the OCABC. Especially, the most common used one-parameter log-linear refractivity model is replaced by the four-parameter one [11] owing to its potential drawback in describing the evaporation duct environment. That is to say, the four characteristic parameters in the vector $\boldsymbol{m} = (d, \Delta M, \rho_1, \rho_2)$ of evaporation duct need to be estimated. The parameter settings for OCABC in the evaporation duct estimation are presented as follows: the population size is 60, the number of food sources is 30, the parameter *limit* is 25, the OC is executed five times at each generation, the maximum number of function evaluations (FEs) is 6000 in each run for a fair comparison, the $L_9(3^4)$ OA is adopted, and the estimated profile is obtained with averagely 10 independent runs. In addition, the radar system parameters are identical to Ref. [9].

Figure 2 shows the comparison of the estimated refractivity profiles obtained by CLPSO, OGABC, and OCABC with the

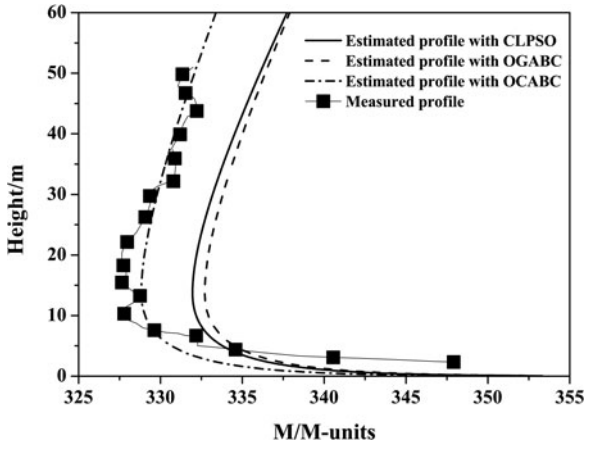

Fig. 2. The comparison of the estimated refractivity profiles with the measured one.

https://doi.org/10.1017/S1759078718000247 Published online by Cambridge University Press

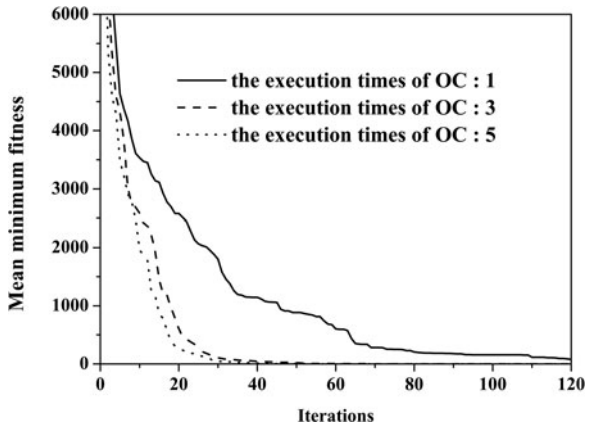

Fig. 3. The convergence progresses with different execution times of OC.

measured one. It can be observed from Fig. 2 that the estimation profile obtained by the OCABC matches well with the measured one compared with the CLPSO and OGABC.

Then, we apply the OCABC to the surface duct estimation with the simulated radar clutter power obtained by the split-step Fourier solution of parabolic equation to further test the stability and accuracy. As you know, the surface duct is commonly represented by the four-parameter refractivity profile, namely, the four characteristic parameters $\boldsymbol{m} = (c_1, c_2, h_1, h_2)$ of surface duct also need to be estimated. The search range of surface duct is defined by: $0 \le c_1 \le 0.25, -3.5 \le c_2 \le -1.0,\ 25.0 \le h_1 \le 50.0,\ 10.0 \le h_2 \le 30.0$. In simulations, the radar works at a frequency of 10 GHz, antenna height of 7 m, power of 91.4 dBm, antenna gain of 52.8 dB, 600 m range bin, beam width of 0.7°, and HH polarization (Horizontal transmit and Horizontal receive). Besides, the radar clutter power simulated by the profile vector $\boldsymbol{m} = (0.13, -2.5, 40, 20)$ is treated as the observed radar clutter power. The Gaussian noise with zero mean is taken into account in the simulated radar clutter power to add the fluctuation to it, and the standard deviation denotes the noise level. The most parameter settings used in OCABC for the surface duct estimation are the same as those given above except for the number of iterations which is 120 and all the estimation results are obtained based on 30 independent runs for each algorithm. Owing to the execution times of OC is of crucial importance to the performance of OCABC. Thus, we will explain how to determine the execution times of OC in the following.

Figure 3 gives the comparison of the convergence progresses with different execution times of OC in the case of without noise. It can be seen that the convergence speed is significantly improved with the increasing number of the execution times of OC, and the difference of the convergence progresses between three and five times is not clear. However, the convergence progress with five times is slightly faster than that of the three times. For this reason, the OC is executed five times at each generation.

To study the convergence performance of the proposed OCABC, the convergence progresses of OCABC are compared with those of the CLPSO and OGABC, and their convergence progresses are plotted in Fig. 4. We can see from Fig. 4 that

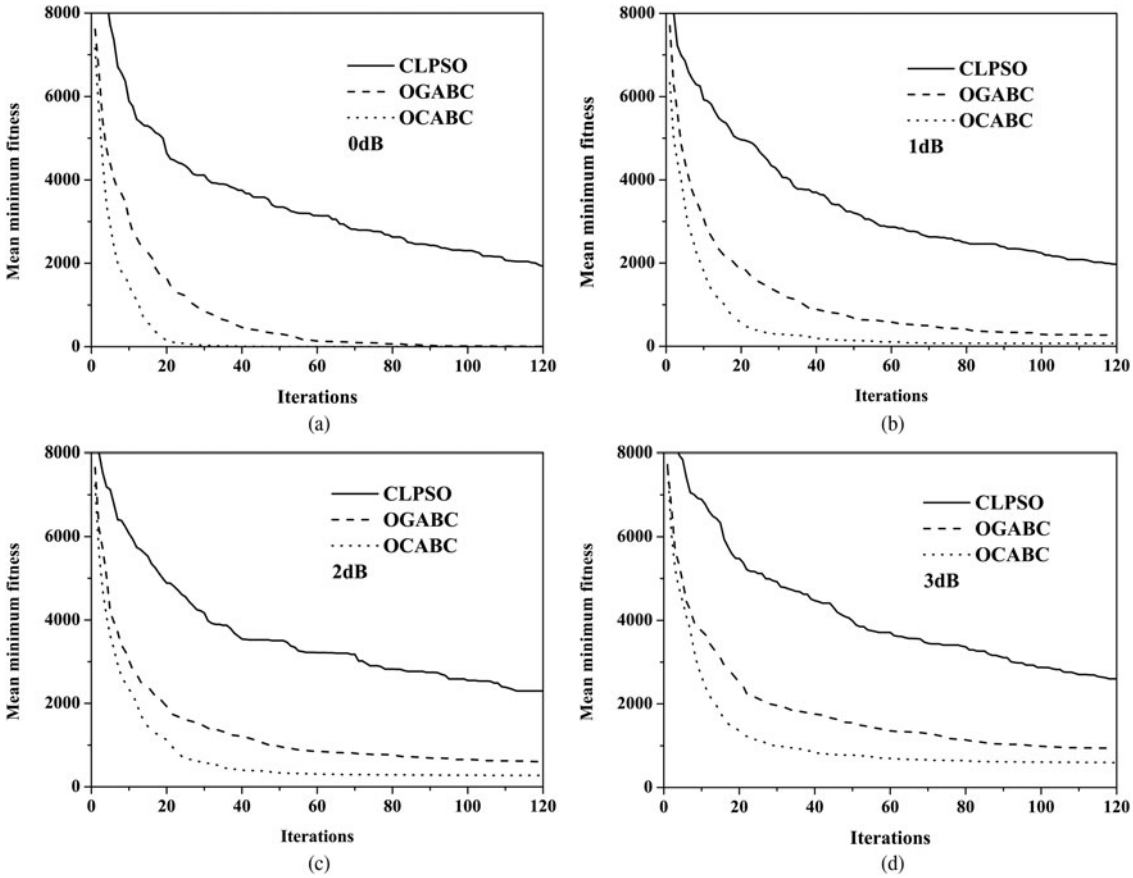

Fig. 4. The comparison of the convergence progresses of CLPSO, OGABC, and OCABC regarding the iterations for the same noise level. (a) 0 dB; (b) 1 dB; (c) 2 dB; (d) 3 dB.

https://doi.org/10.1017/S1759078718000247 Published online by Cambridge University Press

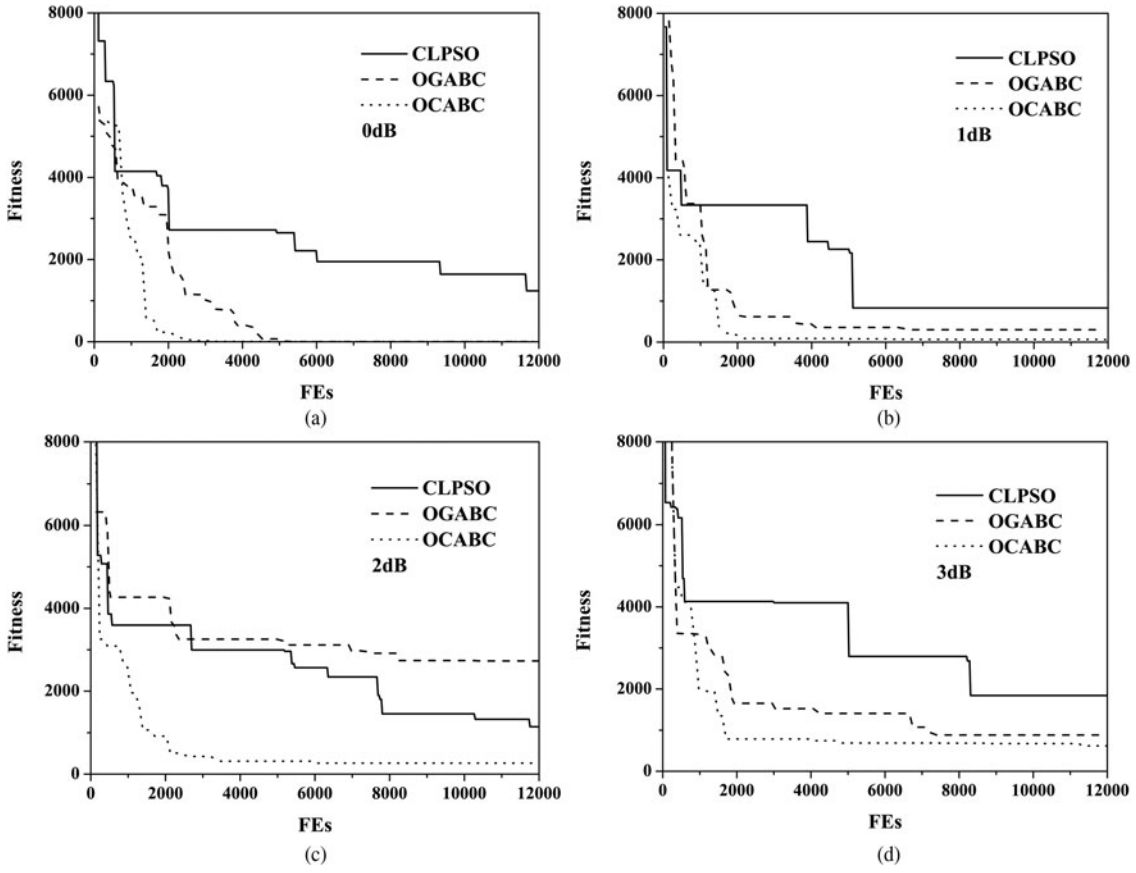

Fig. 5. The comparison of the convergence curves of CLPSO, OGABC, and OCABC regarding the function evaluations with the same noise level. (a) 0 dB; (b) 1 dB; (c) 2 dB; (d) 3 dB.

OCABC is noticeably faster than CLPSO and OGABC for any noise level. In addition, the OCABC can reach the lowest or the same mean minimum fitness value at a high convergence speed. This may be due to the fact that the global best solution in the transmission vector equation not only strengthen the exploitation ability but also accelerate convergence, and the OC operator can

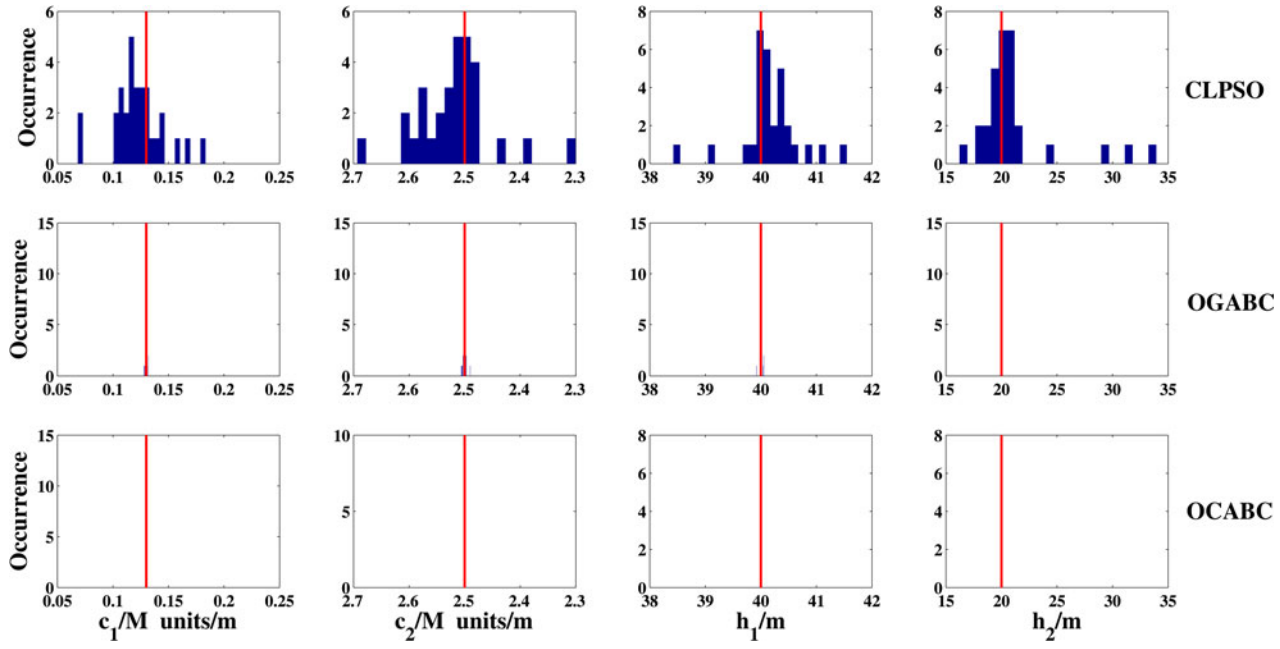

Fig. 6. The comparison of the histograms of CLPSO, OGABC, and OCABC with the noise level of 0 dB.

https://doi.org/10.1017/S1759078718000247 Published online by Cambridge University Press

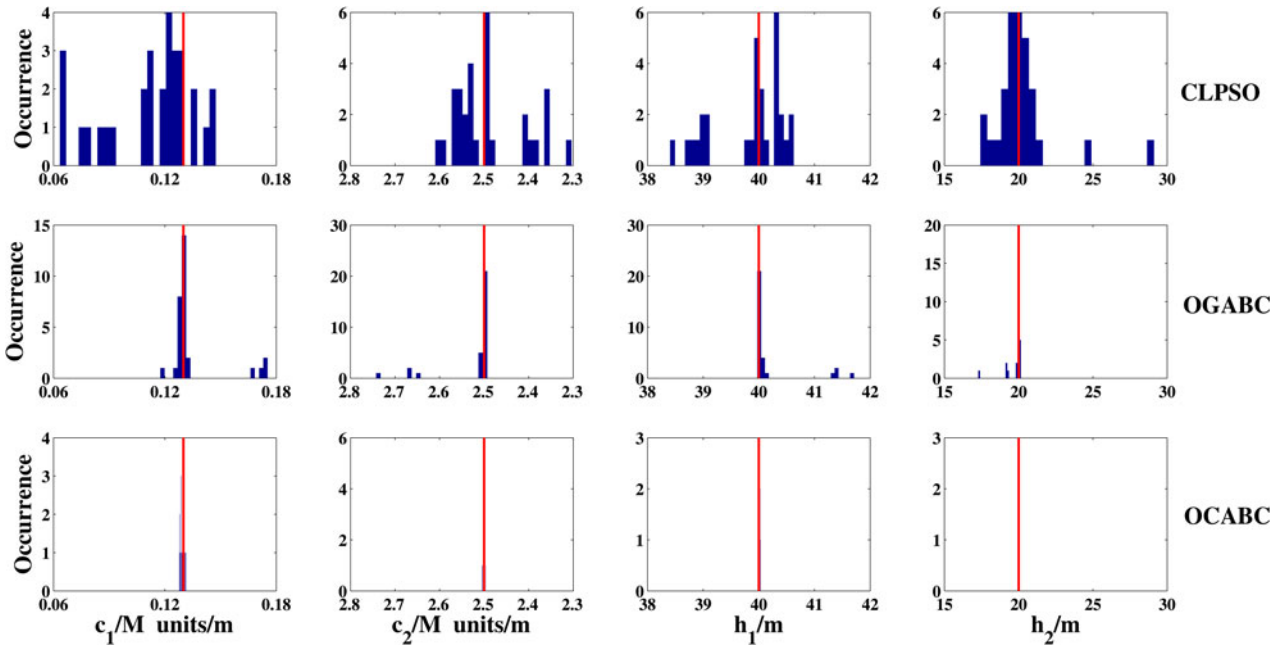

Fig. 7. The comparison of the histograms of CLPSO, OGABC, and OCABC with the noise level of 1 dB.

extract useful information from their previous search experiences to produce a better candidate solution.

Furthermore, the optimization mechanism of the algorithms seems to be different; all the algorithms are further verified by the same maximum number of FEs 12000 in each run for a fair comparison, and the convergence curves are obtained based on a randomly selected run due to the number of FEs of each iteration is changed randomly during the optimization process, and the other parameters of algorithms for the surface duct estimation are consistent with those given above.

The comparison of the convergence curves of CLPSO, OGABC, and OCABC with respect to the number of FEs is presented in Fig. 5. From the results, it is obvious that the convergence speed of OCABC is still much better than those of the other two algorithms, and the OCABC can achieve best fitness value and overcome the disadvantage of trapping into local optima.

A further comparative analysis of the accuracy and stability based on 30 independent runs for the surface duct estimation are provided in the subsequent section. Figures 6–9 exhibit the

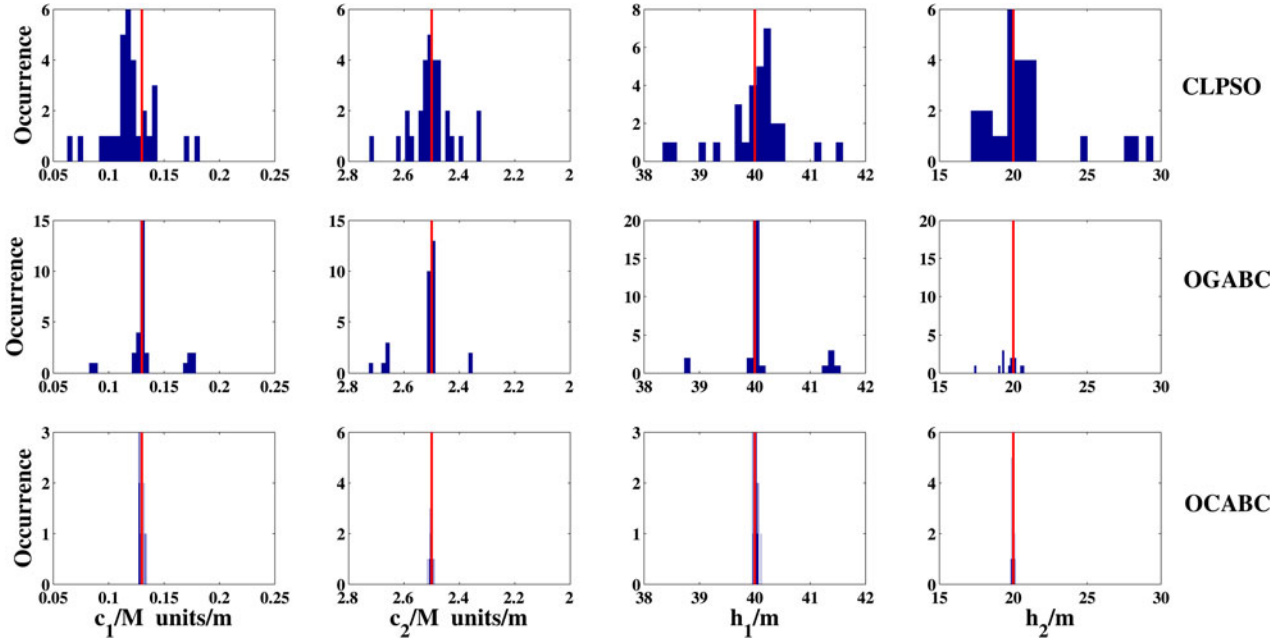

Fig. 8. The comparison of the histograms of CLPSO, OGABC, and OCABC with the noise level of 2 dB.

https://doi.org/10.1017/S1759078718000247 Published online by Cambridge University Press

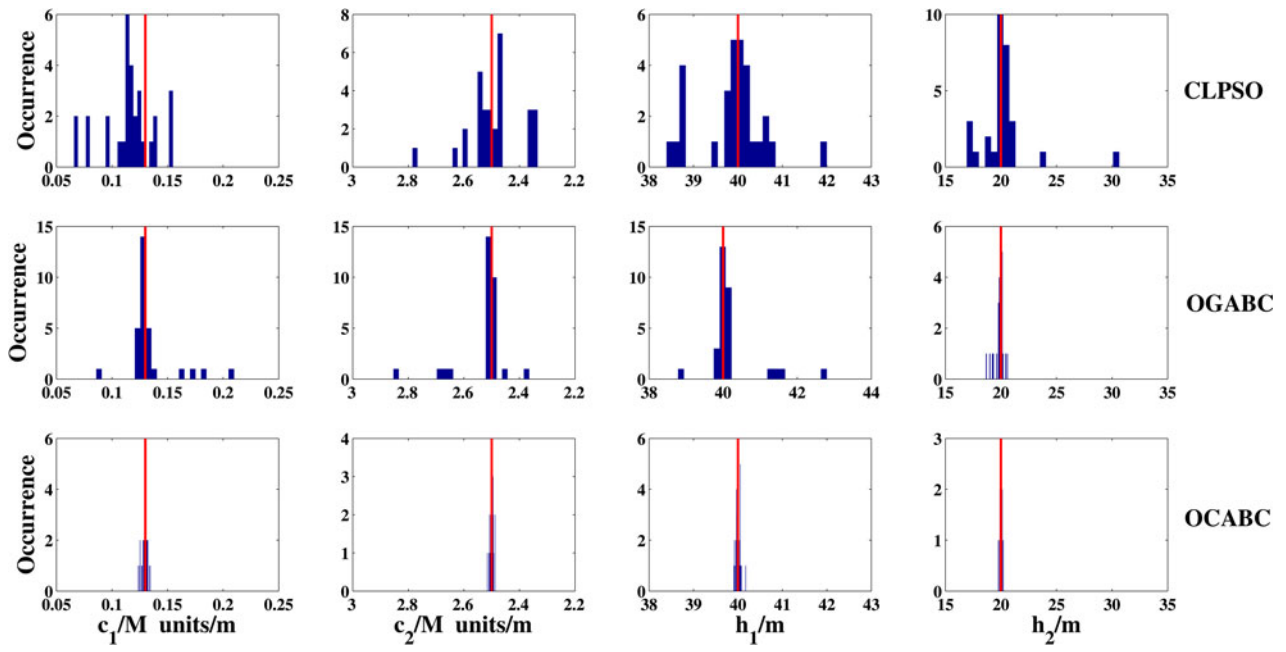

Fig. 9. The comparison of the histograms of CLPSO, OGABC, and OCABC with the noise level of 3 dB.

comparison of the histograms of the estimation results obtained by CLPSO, OGABC, and OCABC with the same noise level, where the red lines represent the position of real parameter of surface duct. It can be observed that the accuracy and stability of OCABC and OGABC are much higher than that of CLPSO in all cases. Both of the OCABC and OGABC almost obtain the same results in the case of without noise. Although the local optima appear in OGABC with the increasing of the noise level, the OCABC still perform well on accuracy and stability. This is caused by the fact that the OC not only can improve the poor exploitation ability of ABC but also make a balance between the exploration ability and exploitation ability, which help ABC to jump out of the local optima.

The corresponding statistical analysis are given in Table 1, and the best results in Table 1 are marked in boldface. It can be clearly observed that the estimation results of OCABC for different noise level are superior to those of CLPSO and OGABC regarding the mean squared error (MSE) defined in Ref. [25], which also quantitatively indicate that the accuracy and stability of OCABC are better than those of CLPSO and OGABC.

Conclusion

Owing to the search equation in ABC is good at exploration but poor at exploitation, an improved ABC algorithm named OCABC based on OED is presented by incorporating the OC and a novel

Table 1. The comparison of the statistical results of CLPSO, OGABC, and OCABC

Noise level	Algorithm	MSE			
		c_1	c_2	h_1	h_2
0 dB	CLPSO	5.74×10^{-4}	0.0050	0.32030	15.398
	OGABC	6.90×10^{-7}	7.315×10^{-6}	4.784×10^{-4}	0.0011
	OCABC	$\mathbf{1.52} \times 10^{-12}$	$\mathbf{1.10} \times 10^{-11}$	$\mathbf{2.03} \times 10^{-10}$	$\mathbf{1.06} \times 10^{-9}$
1 dB	CLPSO	8.863×10^{-4}	0.0065	0.4200	4.3214
	OGABC	2.453×10^{-4}	0.0045	0.2836	0.3068
	OCABC	$\mathbf{1.026} \times 10^{-6}$	$\mathbf{2.938} \times 10^{-6}$	$\mathbf{2.282} \times 10^{-4}$	**0.0012**
2 dB	CLPSO	6.257×10^{-4}	0.0059	0.3801	9.4880
	OGABC	4.579×10^{-4}	0.0066	0.4360	0.3391
	OCABC	$\mathbf{4.174} \times 10^{-6}$	$\mathbf{2.88} \times 10^{-5}$	**0.0018**	**0.0076**
3 dB	CLPSO	6.909×10^{-4}	0.0088	0.5588	5.5452
	OGABC	4.834×10^{-4}	0.0077	0.5165	0.1654
	OCABC	$\mathbf{6.789} \times 10^{-6}$	$\mathbf{4.58} \times 10^{-5}$	**0.0032**	**0.0142**

https://doi.org/10.1017/S1759078718000247 Published online by Cambridge University Press

transmission vector into ABC. In OCABC, the global best solution in the transmission vector can not only strengthen the exploitation ability but also accelerate convergence, and the OC operator can extract useful information from their previous search experiences to produce an excellent candidate solution. The measured and simulated clutter power are utilized to validate the accuracy and effectiveness of the proposed OCABC. The comparative results demonstrate that the performance of the OCABC is superior to that of CLPSO and OGABC for the atmospheric duct estimation.

Acknowledgement. This work was supported by the Young Scientists Fund of the National Natural Science Foundation of China under grant number 61302050.

References

[1] **Yardim C, Gerstoft P and Hodgkiss WS** (2008) Tracking refractivity from clutter using Kalman and particle filters. *IEEE Transactions on Antennas and Propagation* **56**, 1058–1070.

[2] **Yardim C, Gerstoft P and Hodgkiss WS** (2009) Sensitivity analysis and performance estimation of refractivity from clutter techniques. *Radio Science* **44**, RS1008.

[3] **Rogers LT, Hattan CP and Stapleton JK** (2000) Estimating evaporation duct heights from radar sea echo. *Radio Science* **35**, 955–966.

[4] **Gerstoft P, Rogers LT, Krolik LL and Hodgkiss WS** (2003) Inversion for refractivity parameters from radar sea clutter. *Radio Science* **38**, 8053.

[5] **Karimian A, Yardim C, Gerstoft P, Hodgkiss WS and Barrios AE** (2011) Refractivity estimation from sea clutter: an invited review. *Radio Science* **46**, RS6013.

[6] **Yardim C, Gerstoft P and Hodgkiss WS** (2006) Estimation of radio refractivity from radar clutter using Bayesian Monte Carlo analysis. *IEEE Transactions on Antennas and Propagation* **54**, 1318–1327.

[7] **Vasudevan S, Anderson RH, Kraut S, Gerstoft P, Rogers LT and Krolik JL** (2007) Recursive Bayesian electromagnetic refractivity estimation from radar sea clutter. *Radio Science* **42**, RS2014.

[8] **Douvenot R, Fabbro V, Gerstoft P, Bourlier C and Saillard J** (2008) A duct mapping method using least squares support vector machines. *Radio Science* **43**, RS6005.

[9] **Wang B, Wu ZS, Zhao Z and Wang HG** (2009) Retrieving evaporation duct heights from radar sea clutter using particle swarm optimization (PSO) algorithm. *Progress in Electromagnetic Research M* **9**, 79–91.

[10] **Zhao XF, Huang SX, Xiang J and Shi WL** (2011) Remote sensing of atmospheric duct parameters using simulated annealing. *Chinese Physics B* **20**, 099201.

[11] **Zhang JP, Wu ZS, Zhu QL and Wang B** (2011) A four-parameter M-profile model for the evaporation duct estimation from radar clutter. *Progress in Electromagnetics Research* **114**, 353–368.

[12] **Karaboga D and Basturk B** (2007) A powerful and efficient algorithm for numerical function optimization: artificial bee colony (ABC) algorithm. *Journal of Global Optimization* **39**, 459–471.

[13] **Karaboga D, Gorkemli B, Ozturk C and Karaboga N** (2014) A comprehensive survey: artificial bee colony (ABC) algorithm and applications. *Artificial Intelligence Review* **42**, 21–57.

[14] **Yang C** (2013) Estimation of the atmospheric duct from radar sea clutter using artificial bee colony optimization algorithm. *Progress in Electromagnetics Research* **135**, 183–199.

[15] **Yang C, Zhang JK and Guo LX** (2016) Investigation on the inversion of the atmospheric duct using the artificial bee colony algorithm based on opposition-based learning. *International Journal of Antennas and Propagation* **2016**, 2749035.

[16] **Zhu GP and Kwong S** (2010) Gbest-guided artificial bee colony algorithm for numerical function optimization. *Applied Mathematics and Computation* **217**, 3166–3173.

[17] **Barrios AE** (1994) A terrain parabolic equation model for propagation in the troposphere. *IEEE Transactions on Antennas and Propagation* **42**, 90–98.

[18] **Sirkova I** (2012) Brief review on PE method application to propagation channel modeling in sea environment. *Central European Journal of Engineering* **2**, 19–38.

[19] **Gao WF, Liu SY and Huang LL** (2013) A novel artificial bee colony algorithm based on modified search equation and orthogonal learning. *IEEE Transactions in Cybernetics* **43**, 1011–1024.

[20] **Leung YW and Wang Y** (2001) An orthogonal genetic algorithm with quantization for global numerical optimization. *IEEE Transactions on Evolutionary Computation* **5**, 41–53.

[21] **Zhan ZH, Zhang J, Li Y and Shi YH** (2011) Orthogonal learning particle swarm optimization. *IEEE Transactions on Evolutionary Computation* **15**, 832–847.

[22] **Wang Y, Cai Z and Zhang Q** (2012) Enhancing the search ability of differential evolution through orthogonal crossover. *Information Sciences* **185**, 153–177.

[23] **Xiong G, Shi D and Duan X** (2014) Enhancing the performance of biogeography-based optimization using polyphyletic migration operator and orthogonal learning. *Computers & Operations Research* **41**, 125–139.

[24] **Liang JJ, Qin AK, Suganthan PN and Baskar S** (2006) Comprehensive learning particle swarm optimizer for global optimization of multimodal functions. *IEEE Transactions on Evolutionary Computation* **10**, 281–295.

[25] **Notarnicola C, Angiulli M and Posa F** (2008) Soil moisture retrieval from remotely sensed data: neural network approach versus Bayesian method. *IEEE Transactions on Geoscience and Remote Sensing* **46**, 547–557.

Chao Yang received his Ph.D degree in Radio Physics from Xidian University, Xi'an, China in 2010. He is now an Associate Professor at the School of Science, Xi'an University of Posts and Telecommunications, Xi'an, China. His research interests include electromagnetic wave propagation and scattering in complex and random media, and optimization techniques in electromagnetic problems.

Lixin Guo received the M.S. degree in Radio Science from Xidian University, Xi'an, China, and the Ph.D degree in Astrometry and Celestial Mechanics from Chinese Academy of Sciences, China, in 1993 and 1999, respectively. He is currently a Professor at the School of Physics and Optoelectronic Engineering, Xidian University, China. His research interests include electromagnetic wave propagation and scattering in complex and random media, computational electromagnetics, inverse scattering, antenna analysis and design.

https://doi.org/10.1017/S1759078718000247 Published online by Cambridge University Press